Geophysical Research Letters

RESEARCH LETTER
10.1029/2018GL080424

Key Points:
- Airborne in situ measurements of VOCs with a wide range of lifetimes are used to quantify a convective-transport transit time spectrum
- The transit time scale derived from VOC measurements is broadly comparable to that estimated from convective mass flux
- The estimated transit time spectrum has the potential to serve as an effective diagnostic for evaluating convective transport in CCMs

Correspondence to:
Z. J. Luo and L. L. Pan,
zluo@ccny.cuny.edu;
liwen@ucar.edu

Citation:
Luo, Z. J., Pan, L. L., Atlas, E. L., Chelpon, S. M., Honomichl, S. B., Apel, E. C., et al. (2018). Use of airborne in situ VOC measurements to estimate transit time spectrum: An observation-based diagnostic of convective transport. *Geophysical Research Letters*, *45*. https://doi.org/10.1029/2018GL080424

Received 10 SEP 2018
Accepted 20 NOV 2018
Accepted article online 29 NOV 2018

Use of Airborne In Situ VOC Measurements to Estimate Transit Time Spectrum: An Observation-Based Diagnostic of Convective Transport

Zhengzhao Johnny Luo[1], Laura L. Pan[2], Elliot L. Atlas[3], Sofia M. Chelpon[4], Shawn B. Honomichl[2], Eric C. Apel[2], Rebecca S. Hornbrook[2], and Samuel R. Hall[2]

[1]Department of Earth and Atmospheric Sciences, City College of City University of New York (CUNY), New York, NY, USA, [2]Atmospheric Chemistry Observations and Modeling Laboratory, National Center for Atmospheric Research, Boulder, CO, USA, [3]Department of Atmospheric Sciences, University of Miami, Coral Gables, FL, USA, [4]Program in Earth and Environmental Sciences, Graduate Center, City University of New York (CUNY), New York, NY, USA

Abstract Convective transport from the marine boundary layer to the upper troposphere (UT) is investigated using airborne in situ measurements of chemical species over the tropical western Pacific. Using 42 volatile organic compounds with photochemical lifetimes ranging from shorter than a day to multiple decades, we derive a transit time spectrum *G(t)* and the associated modal and mean transit times for the UT air mass over the convectively dominant tropical western Pacific region. *G(t)* describes relative contributions of air masses transported from the marine boundary layer to the UT via all transport paths with different transit times. We further demonstrate that the volatile organic compound-derived transit time scale is broadly comparable to that estimated from convective mass flux. The observation-based transit time spectrum not only provides insights into convective transport pathways, but also has the potential to serve as an effective diagnostic for evaluating the representation of convective transport in global models.

Plain Language Summary Tropical deep convection is an important mechanism whereby air mass and chemical species are transported from near the surface to the upper troposphere and lower stratosphere. This transport process is difficult to quantify by observations or represent in models because of the small spatial scales and short temporal scales involved. In this study, we present a method to characterize convective transport using the framework of transit time spectrum, which describes the relative contributions of different transport paths with different transit times. We demonstrate that convective transport transit time spectrum can be derived using airborne in situ measurements of chemical species with a wide range of lifetimes, and we illustrate the wealth of information they provide for quantifying transport processes. This analysis method has the potential to serve as a unique diagnostic for evaluating the representation of convective transport in global models.

1. Introduction

Tropical deep convection plays a crucial role in transporting near-surface air into the upper troposphere (UT), which not only affects the vertical distribution of heat and moisture (Johnson et al., 2016; Yanai et al., 1973), but also effectively redistributes chemically active species between the boundary layer and the UT to modify the chemical environment of the UT (e.g., Pan et al., 2017). Accurately representing convective transport in global chemistry climate models (CCMs) is important for understanding and quantifying its role in chemistry-climate interaction. However, it has been a long-standing challenge for global models to adequately represent convection due to the fact that convection is typically a subgrid scale phenomenon that is not treated explicitly but has to be parameterized (Arakawa, 2004).

Evaluating the model representation of convective transport in reproducing the observed chemical distribution, especially the presence of very short-lived (VSL) species (defined as the species with lifetime under 6 months) in the UT and lower stratosphere (UTLS), is a significant ongoing activity (e.g., Hossaini et al., 2010; Orbe et al., 2018; Ordonez et al., 2012; Wales et al., 2018). A number of large field campaigns in recent years have focused on the impacts of convection on chemical composition (e.g., Barth et al., 2015; Pan et al., 2017; Toon et al., 2016). These new observations not only challenge the ability of CCMs to represent the observed convection-driven chemical environment, but also present unprecedented opportunities for

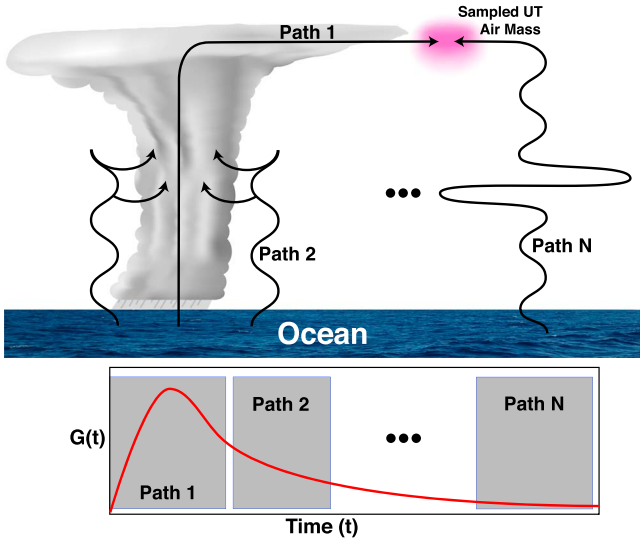

Figure 1. Schematic of transport paths in the convectively dominant tropical western Pacific. A transit time spectrum, *G(t)*, is defined to describe the relative contributions of these different paths. UT = upper troposphere.

creating new observation-based diagnostics. In this letter, we demonstrate the use of airborne in situ measurements to produce an observation-based transit time spectrum and discuss its applications as a diagnostic for models.

The concept and the mathematical framework of the "transit time spectrum" have a long history. In particular, the concept of "age of air" has been widely used in the stratospheric community to characterize transport, perform model evaluations, and compare model predictions with observations (Hall & Plumb, 1994; Waugh & Hall, 2002, and references therein). While it can be relatively straightforward to determine the mean age of an air mass using trace gas observations, deriving an age spectrum (or transit time spectrum) is much more difficult (Ehhalt et al., 2007; Schoeberl et al., 2000, 2005). Although this framework has been applied to tropospheric transport in recent years, most of these studies focus on using passive tracers in models to characterize the contribution of various source regions to the global atmosphere (e.g., Holzer & Hall, 2000; Holzer & Waugh, 2015; Konopka et al., 2017; Orbe et al., 2013).

In this work, we demonstrate a method of using volatile organic compound (VOC) observations to derive a transit time spectrum associated with convective transport over the tropical western Pacific (TWP) warm pool, utilizing airborne in situ data from the CONvective Transport of Active Species in the Tropics (CONTRAST) experiment (Pan et al., 2017). Our method expands on the work of Schoeberl et al. (2005) who used chemical species measurements to constrain the stratospheric age spectrum. Over the TWP, widespread and intense deep convection couples the oceanic, biochemically produced VSL organic halogens to the UTLS, where they play important roles in ozone chemistry. In contrast to the stratospheric transport where the time scale is months to years, the convective transport time scale from the marine boundary layer (MBL) to the UTLS is hours to days. Accurately representing convective transport in this region is a significant challenge for the CCMs.

In Figure 1, we use a schematic drawing to illustrate the concept of transit time spectrum in this highly convective environment. Here the fastest transport path (Path 1) is direct pumping of MBL air by deep convection. Deep convection also entrains a large amount of air from the surrounding environment (Houze, 1993, 2014; Luo et al., 2010); the convective entrainment process is depicted by Path 2. Additional transport pathways (Path N, where $N \geq 3$) involve different amounts of horizontal motion and slow ascent outside of active convection but still in the convectively disturbed environment where mean vertical motion is generally upward. The transit time spectrum therefore describes the probability distribution of the various transport pathways the UT air mass has experienced.

The main objective of this letter is to introduce the method of analysis and demonstrate the wealth of information contained in the distribution of chemical compounds for quantifying transport, especially in the region dominated by the convective transport.

2. Trace Gas Measurements During CONTRAST

The CONTRAST experiment was conducted from Guam (13.5°N, 144.8°E) in January–February 2014 using the National Science Foundation/National Center for Atmospheric Research Gulfstream V (GV) research aircraft (Pan et al., 2017). Primary goals of the CONTRAST experiment include characterizing the influence of deep convection on the chemical composition of the tropical UTLS and investigating transport pathways from the ocean surface to the tropopause. Two instruments onboard the GV aircraft are most relevant to the current study: the Trace Organic Gas Analyzer (TOGA, Apel et al., 2012) and the Advanced Whole Air Sampler (AWAS, https://www.eol.ucar.edu/instruments/advanced-whole-air-sampler). Both instruments obtained measurements of a large suite of VOCs of natural and anthropogenic emission sources (Pan et al., 2017). Analyses using these data have quantified a number of key aspects of the region's chemical environment (Anderson et al., 2017; Chen et al., 2016; Koenig et al., 2017; Nicely et al., 2016; Wales et al., 2018). Examples of CONTRAST data and vertical sampling can be found in these works. In this study, a total of 42

Table 1
VOCs and Tropospheric Lifetimes Used to Generate the Transit Time Spectrum

ID	Instrument	VOC	Lifetime [days]	Source of estimate
1	TOGA	Acetaldehyde, CH_3CHO	0.25	Calculated
2	AWAS	DMS, $(CH_3)_2S$	0.96	Calculated
3	AWAS	n-Pentane, C_5H_{12}	1.2	Calculated
4	TOGA, AWAS	n-Butane, C_4H_{10}	1.9	Calculated
5	TOGA, AWAS	Isobutane, $CH(CH_3)_3$	2.1	Calculated
6	AWAS	n-Butyl Nitrate, $C_4H_9ONO_2$	2.2	Calculated
7	AWAS	2-Butyl Nitrate, $C_2H_5CH(CH_3)ONO_2$	3.8	Calculated
8	TOGA, AWAS	Benzene, C_6H_6	3.8	Calculated
9	TOGA, AWAS	Propane, C_3H_8	4.2	Calculated
10	TOGA	Methanol, CH_3OH	5.2	Calculated
11	AWAS	Ethyne, C_2H_2	6.0	Calculated
12	AWAS	Isopropyl Nitrate, $CH(CH_3)_2ONO_2$	6.4	Calculated
13	AWAS	Chlorobenzene, C_6H_5Cl	9.2	Calculated
14	AWAS	Ethyl Nitrate, $C_2H_5ONO_2$	11	Calculated
15	TOGA, AWAS	Bromoform, $CHBr_3$	13	Calculated
16	AWAS	Dibromochloromethane, $CHBr_2Cl$	13	Calculated
17	AWAS	1,2-Dichloroethane, CH_2ClCH_2Cl	16	Calculated
18	AWAS	Ethane, C_2H_6	18	Calculated
19	TOGA, AWAS	Tetrachloroethylene, C_2Cl_4	27	Calculated
20	AWAS	Bromodichloromethane, $CHBrCl_2$	37	Calculated
21	TOGA, AWAS	Dibromomethane, CH_2Br_2	39	Calculated
22	AWAS	Bromochloromethane, CH_2BrCl	40	Calculated
23	TOGA, AWAS	Dichloromethane, CH_2Cl_2	44	Calculated
24	TOGA, AWAS	Chloroform, $CHCl_3$	48	Calculated
25	AWAS	Methyl Chloride, CH_3Cl	120	Calculated
26	AWAS	Methyl Bromide, CH_3Br	150	Calculated
27	AWAS	Methyl Chloroform, CH_3CCl_3	450	Calculated
28	AWAS	HFC-365mfc, $C_4H_5F_5$	620	Calculated
29	AWAS	HCFC-141b, $C_2H_3Cl_2F$	760	Calculated
30	AWAS	HCFC-22, $CHClF_2$	980	Calculated
31	AWAS	HCFC-134a, $C_2H_2F_4$	1,100	Calculated
32	AWAS	HCFC-142b, $C_2H_3ClF_2$	1,700	Calculated
33	AWAS	Carbonyl Sulfide, OCS	2,000	Johnson (1981)
34	AWAS	Halon 1211, $CBrClF_2$	5,800	SPARC Report No. 6
35	AWAS	Halon 2402, $CBrF_4$	10,000	SPARC Report No. 6
36	TOGA, AWAS	Carbon Tetrachloride, CCl_4	12,000	SPARC Report No. 6
37	AWAS	CFC-112a, $C_2Cl_4F_2$	19,000	Carpenter et al. (2014)
38	AWAS	CFC-11, CCl_3F	19,000	SPARC Report No. 7
39	AWAS	CFC-112, $C_2Cl_4F_2$	22,000	Carpenter et al. (2014)
40	AWAS	CFC-113, $C_2Cl_3F_3$	34,000	SPARC Report No. 6
41	AWAS	CFC-12, CCl_2F_2	37,000	SPARC Report No. 6
42	AWAS	CFC-114, $C_2Cl_2F_4$	69,000	SPARC Report No. 6

Note. Only two significant figures are kept for the VOC lifetimes. The last column gives the sources from which we obtain the estimates of VOC lifetimes. VOC = volatile organic compound; TOGA = Trace Organic Gas Analyzer; AWAS = Advanced Whole Air Sampler.

trace gases from TOGA and AWAS are used (Table 1). All species involved are emitted into the boundary layer and are lost in the troposphere through photochemical reactions.

As shown in Table 1, the selected trace gas species have photochemical lifetimes ranging from a few hours to a few decades. Note that the photochemical lifetime is a variable that depends on the chemical and radiative environment the air mass experiences in the process of transport. A key approximation we make in this work is to use a constant lifetime for each tracer and assume this estimated lifetime adequately represents the chemical loss rate during the transport.

The lifetimes listed in Table 1 are estimated as follows. For the first 32 species (No. 1 – No. 32), the tracer lifetimes are calculated using temperature-dependent rate constants from the NIST compilation (Manion et al., 2015) and OH concentrations in the CONTRAST region calculated by a constrained chemical box

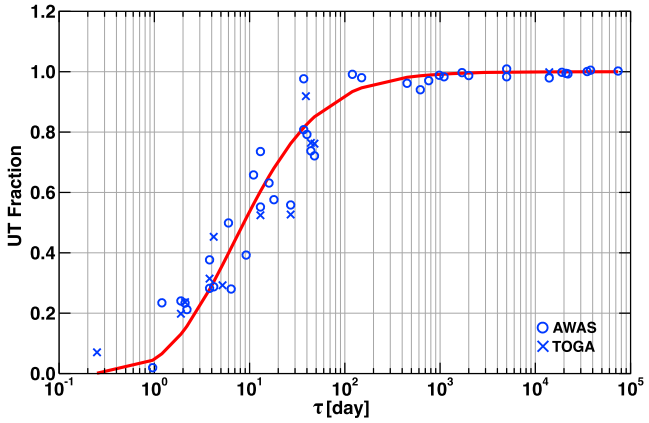

Figure 2. UT fraction (μ^*) versus lifetime (τ) derived from the CONTRAST observations (crosses for TOGA data and circles for AWAS data). The red curve shows the nonlinear least squares fit to the data. Detail of data fitting is described in the text. UT = upper troposphere; TOGA = Trace Organic Gas Analyzer; AWAS = Advanced Whole Air Sampler.

model by Nicely et al. (2016). The median temperature of the MBL observed by GV and the median 24-hr average OH concentration estimated for the CONTRAST field campaign are used in the calculations. Lifetimes of the species dominated by photolysis loss are estimated from the TUV model (http://cprm.acom.ucar.edu/Models/TUV/Interactive_TUV/) and measurements from the GV (Hall, 2015) within ±2 hr of local noon, scaled by an appropriate factor (0.25–0.3) to estimate 24-hr average conditions. Global lifetimes for longer-lived species (No. 33–No. 42) are compiled from published literatures (Carpenter et al., 2014; Johnson, 1981; SPARC, 2013, 2016).

3. Determination of the Transit Time Spectrum

Over the TWP warm pool, trace gas concentration in the UT is closely connected to that in the MBL because of the prevalence of deep convection (e.g., Krysztofiak et al., 2018; Pan et al., 2017). Conceptually, we expect the presence of the short-lived species in the UT to be dominated by the convective pumping from the regional MBL (Path 1 in Figure 1). The longer-lived species, on the other hand, tend to be uniformly mixed in the troposphere through a variety of transport pathways. If the vertical transport by convection is the dominant process, the species' UT fraction, that is, the mixing ratio in the UT divided by that in the MBL, should show a relatively compact relationship with the species' lifetimes (τ). This relationship derived from the CONTRAST data and the estimated lifetimes (Table 1) is shown in Figure 2, where the UT fractions (μ^*) are calculated using the average mixing ratios observed in the 12–14 km layer (UT) and the 0–2 km layer (MBL). The 12–14 km layer is chosen to represent the convective transport dominated UT, which is consistent with CloudSat observations of the predominant convective outflow layer of the region (Pan et al., 2017; Takahashi & Luo, 2012). The 0–2 km layer is used to approximately represent the MBL as the convective transport origin. To limit our analysis to the TWP warm pool, only data collected within 0–20°N and 130–170°E are included.

The μ^*-τ relationship provides a number of insights for the transport processes in the region. Foremost, the compact relationship supports the conceptual model and the hypothesis that the UT fractions of the selected tracers are dominated by the convective-driven vertical transport that closely links the MBL and the UT (Figure 1). Quantitatively, μ^* increases with τ and asymptotes to unity for $\tau > 3$ months to a year, which indicates that fast convective transport primarily controls the amount of VSL species in the UT. The longer-lived species are already well mixed vertically and convective transport has little impact. The observed μ^* are therefore near unity for the longer-lived species. That the CONTRAST VOC measurements provide sufficient coverage of lifetime range to map out the shorter-lived species and produce a fairly compact μ^*-τ relationship is a strong motivation for this study.

Based on the conceptual framework illustrated in Figure 1 and the observed μ^*-τ relationship in Figure 2, we take the following steps to derive the transit time spectrum using this set of observations. Under the approximation of constant lifetime, the evolution of the trace gas mixing ratio following its local emission or after its transport to the local boundary layer can be represented by an exponential decay (Ehhalt et al., 2007; Schoeberl et al., 2000, 2005):

$$m_i(t) = m_i(0)e^{-t/\tau_i}, \tag{1}$$

where t is the transit time (initial $t = 0$), i is tracer index, and τ_i is the estimated tracer lifetime. Since an air mass at the point of sampling (X_s) consists of a mixture of air parcels that are transported from the points of origin through paths associated with various transit times, the mixing ratio of a particular VOC at the point of sampling, $m_{is}(X_s)$, is an average of all possible contributions, weighted by the transit time spectrum. Under the approximation of a steady state and a homogeneous boundary condition, the result is represented by

$$m_{is}(X_s) = m_{io}\int_0^\infty e^{-t/\tau_i} G(X_s, t)dt, \tag{2}$$

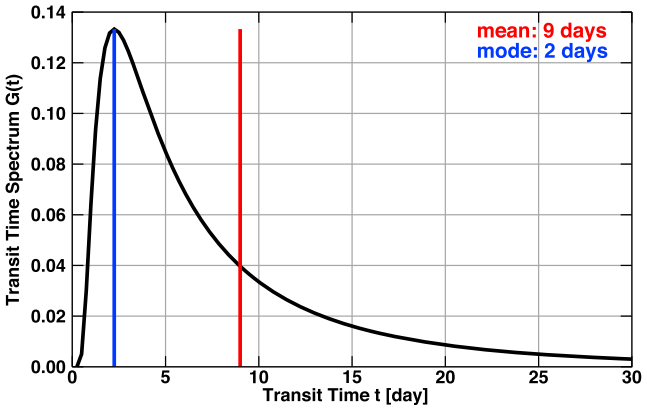

Figure 3. Estimated transit time spectrum, *G(t)*, for the UT (12–14 km) air mass sampled during the CONTRAST experiment in the tropical western Pacific warm pool.

where m_{io} is the MBL source mixing ratio of specie i, $G(X_s, t)$ is the transit time spectrum, which describes the relative contributions of all possible transport paths from the MBL to the sampling location X_s (see Figure 1). X_s represents the 3-D spatial coordinates of the sampling. In this application, we are mainly interested in the transit time characteristic of a UT layer centered at height z. Hence, equation (2) is further reduced to

$$\mu_i(z) \equiv m_{is}(z)/m_{io} = \int_0^\infty e^{-t/\tau_i} G(z,t)dt, \tag{3}$$

where $\mu_i(z)$ is the UT fraction of trace gas i at level z.

Equation (3) indicates that the species' UT fractions, $\mu_i(z)$, are essentially a Laplace transform of the transit time spectrum under the approximations made in this study. Using the large suite of VOCs observed during CONTRAST, which covers the entire range of relevant transport time scales, the transit time spectrum $G(z,t)$ can, in principle, be derived using an inverse Laplace transform. In practice, however, the matrix inversion involved is numerically unstable. As an alternative, we adopt an approach of using the analytical solution of a one-dimension (1-D) diffusive model, as described in Hall and Plumb (1994), as a constraint for the inversion. In other words, we assume the inversion of equation (3) has the functional form

$$G(z,t) = \frac{z}{2\sqrt{\pi K t^3}} \exp\left(\frac{z}{2H} - \frac{Kt}{4H^2} - \frac{z^2}{4Kt}\right), \tag{4}$$

where H is the scale height of the atmosphere and K is the effective diffusion coefficient in the 1-D model, but here it is a parameter to be constrained by the observations. Note that although equation (4) is the solution for a 1-D model, previous studies of stratospheric age spectrum have shown that the functional form captures the essential characteristics of the age spectrum produced by 3-D transport models (Schoeberl et al., 2000, 2005).

The parameter K in equation (4) can be determined by performing a nonlinear-least-squares fit to the observation by minimizing

$$F = \Sigma_{i=1}^{52} \left(\mu_i - \mu_i^*\right)^2, \tag{5}$$

where μ_i is modeled by equation (3) and μ_i* is the observed UT fractions. Using an iteration method, we obtain the best fit to the observed μ*-τ relationship (symbols in Figure 2) using the average UT fractions of the 52 independent VOC measurements (Table 1). The calculation chooses z to be 13 km (midpoint for the 12–14 km layer), and H to be 7.6 km (for the tropical troposphere). The best fit for the μ*-τ relationship is shown as the red curve in Figure 2. The optimal value of K is 115 m^2/s. The r^2 of the fit is 0.93. Using the optimal K, the transit time spectrum is fully determined and is shown in Figure 3.

Note that although the vertical coordinate, z, is the only explicit spatial variable in equation (3), the derived transit time spectrum is not limited to representing 1-D transport. Conceptually, equation (3) integrates over time along all possible 3-D Lagrangian paths from the source (MBL) to the destination (UT). The 1-D diffusion model solution is introduced only to help constrain the derivation of *G(t)* in this general framework. The specific shape of the curve is fitted to the observations using K as a single parameter. Here K no longer represents the diffusivity of a 1-D system, but is used to parameterize the collective effect of convective transport from the MBL to the UT represented by the specific set of observations. The excellent fit (r^2 = 0.93) is a strong support for this assumption.

The transit time spectrum *G(t)*, which quantifies the relative contributions to the observed UT air mass from various transport paths with different transit times, provides a basis to derive key metrics for quantifying the region's transport time scales. The two most important quantities for the time scales are the modal and the

mean transit times. The former, T_{mod}, is identified by the maximum of $G(t)$, and the latter, $\overline{T}$, is defined as the first moment of the spectrum:

$$\overline{T} \equiv \int_0^\infty tG(t)dt. \quad (6)$$

The derived transit time spectrum shown in Figure 3 has the mode and mean to be 2 and 9 days, respectively. Although the specific values of the transit time scales as reported here are subject to uncertainty and variability, we make a special note that they are distinctly shorter than the stratospheric transit times discussed in previous publications, which are typically years (e.g., Li et al., 2012; Schoeberl et al., 2005) most relevant to long-lived tracers being redistributed between the tropical tropopause and the polar region. In contrast, the transit time spectrum derived here for the tropical troposphere represents an entirely different transport regime, and is especially relevant to the transport of VSL species ($\tau < 6$ months) from the MBL to the UT.

To cast the result in a broader context, we compare the estimated mean transit time (9 days) to the time scale inferred from convective mass flux. In a recent study, Masunaga and Luo (2016) developed a satellite-based algorithm to retrieve convective mass flux and total mass flux. Over the TWP, convective mass flux accounts for a large fraction of the total mass flux, which is estimated to be 0.005–0.015 $kg{\cdot}m^{-2}{\cdot}s^{-1}$. Since mass flux equals air density (ρ_{air}) times the mean vertical velocity ($\overline{w}$), if we use 0.62 kg/m^3 as a representative ρ_{air} for the tropical troposphere, then the estimated $\overline{w}$~0.8–2.4 cm/s. This translates to a mean transit time (from the MBL to UT) of ~6–19 days. Hence, the VOC-derived transit time scale is broadly comparable to that derived from consideration of convective mass flux.

4. Summary and Discussions

Using 52 independent measurements of 42 VOCs with photochemical lifetimes ranging from shorter than a day to multiple decades measured by TOGA and AWAS during the CONTRAST field campaign, we have derived a transit time spectrum $G(t)$, including the modal and mean transit times, for the UT air mass over the convectively dominant TWP region. The result demonstrates the potential of this method to unravel transport information contained in chemical species and the application in the troposphere of a successful method previously used in diagnosing stratospheric transport.

Much research work needs to be done to better understand the uncertainty and limitations of this method. A number of factors contribute to the variabilities and uncertainties of the derived characteristic transit times. First, the representativeness of the samples we use in calculation is a significant factor for the variability. When using the campaign-averaged UT layer mixing ratios, we essentially use the airborne measurements that are most representative of the perturbed background condition of the TWP region. Occasionally, fresh convective outflow was sampled during the campaign, such as the example shown in Figure 8 of Pan et al. (2017). Using the samples that immediately follow convective events, we have found that the estimated mean transit times to be 10–20% shorter. Second, our method assumes that trace gas species measured in the regional MBL is a sufficient representation of the source region of transport (see equation (2)). This could include emission from local source or transport to the regional MBL from elsewhere. However, the source region associated with large-scale quasi-horizontal mixing from regions outside the TWP and influence of the air mass above the MBL are not explicitly accounted for in equation (2), which could introduce uncertainty to the analysis. We do not expect this process to have a significant impact on short-lived species, which are unlikely to survive the long transport time, or long-lived species, which are uniformly distributed, but the impact on species with intermediate lifetime needs to be further investigated. Third, the derived mode and mean of the transit time spectrum are sensitive to the VOC lifetimes used in the calculation, which vary with temperature, altitude, and estimated chemical kinetic factors, including abundance of OH. For demonstration of the concept presented here, we used lifetimes based on the MBL temperature and model estimates of OH concentration. Using lifetimes based on tropospheric column average temperature and OH will result in a set of transit time scales approximately double these values.

Given these considerations, we emphasize that the specific modal and mean values of the spectrum presented in Figure 3 (2 and 9 days) should be considered as approximations for transit time scales associated with convective transport from the MBL to the UT for the region of study. A thorough uncertainty analysis,

involving detailed analyses of sensitivity to the lifetime estimate, to the use of constant lifetimes, to the selection of the VOCs, to spatial sampling choices, and other factors is in progress to be reported in follow-up papers.

The observation-based transit time spectrum not only provides a metric to quantify regional transport characteristics, but it also has the potential to serve as a diagnostic for evaluating and improving the representation of convective transport in models. A transit time spectrum for the same region can be estimated using Lagrangian back trajectory analyses (e.g., Bergman et al., 2013; Schoeberl et al., 2000). Comparing the resulting spectrum with the result from this work will shed light on how well the vertical motion in convectively dominated region is represented in various meteorological analyses or reanalyses data sets. Representation of convective transport in CCMs can be evaluated by comparing the transit time spectra derived from modeled VOCs or idealized time-decaying tracers with that derived from observations using the same method as presented in this study. Comparisons can also be made with the results from studies that use approaches of releasing passive, pulse tracers from the boundary layer (e.g., Li et al., 2012; Ploeger & Birner, 2016). Our ongoing research seeks to apply these approaches to the Whole Atmosphere Community Climate Model simulations which include both artificial tracers and an extensive list of chemical species with lifetimes that span the relevant transport time scales.

Finally, we note that a critical gap exists between observations of convection and its parameterization in global models: while global observations of convection focus on measuring atmospheric hydrometers such as clouds and precipitation (Stephens, 2005), formulation of convection parameterizations are largely based on convective dynamics that uses concepts such as convective mass flux (Arakawa, 2004). The convective transport transit time spectrum based on redistribution of chemical species will add a new dimension of information content for diagnosing the representation of convective dynamics in models.

Acknowledgments
Funding for this work was provided in part by NCAR ACOM Laboratory, advanced study program, and visitor program, and in part by NASA grant to CUNY (80NSSC17K0197). We thank members of CONTRAST science team for the flight operation and data. The CONTRAST experiment and NCAR are sponsored by NSF. EA acknowledges funding by NSF Grant AGS1261657, and thanks S. Schauffler, V. Donets, R. Lueb, L. Pope, M. Navarro, and X. Zhu for contributions to sample collection and analysis. Z.J.L. thanks William B. Rossow and Yutian Wu for helpful comments. CONTRAST data are publicly available for all researchers and can be obtained at https://data.eol.ucar.edu/master_list/?project=CONTRAST.

References

Anderson, D. C., Nicely, J. M., Wolfe, G. M., Hanisco, T. F., Salawitch, R. J., Canty, T. P., et al. (2017). Formaldehyde in the tropical western Pacific: Chemical sources and sinks, convective transport, and representation in CAM-Chem and the CCMI models. *Journal of Geophysical Research: Atmospheres*, *122*, 11,201–11,226. https://doi.org/10.1002/2016JD026121

Apel, E. C., Olson, J. R., Crawford, J. H., Hornbrook, R. S., Hills, A. J., Cantrell, C. A., et al. (2012). Impact of the deep convection of isoprene and other reactive trace species on radicals and ozone in the upper troposphere. *Atmospheric Chemistry and Physics*, *12*(2), 1135–1150. https://doi.org/10.5194/acp-12-1135-2012

Arakawa, A. (2004). The cumulus parameterization problem: Past, present, and future. *Journal of Climate*, *17*, 2493–2525. https://doi.org/10.1175/1520-0442(2004)017<2493:RATCPP>2.0.CO;2

Barth, M. C., Cantrell, C. A., Brune, W. H., Rutledge, S. A., Crawford, J. H., Huntrieser, H., et al. (2015). The deep convective clouds and chemistry (DC3) field experiment. *Bulletin of the American Meteorological Society*, *96*, 1281–1309. https://doi.org/10.1175/BAMS-D-13-00290.1

Bergman, J. W., Fierli, F., Jensen, E. J., Honomichl, S., & Pan, L. L. (2013). Boundary layer sources for the Asian anticyclone: Regional contributions to a vertical conduit. *Journal of Geophysical Research: Atmospheres*, *118*, 2560–2575. https://doi.org/10.1002/jgrd.50142

Carpenter, L. J., Reimann, S., Burkholder, J. B., Clerbaux, C., Hall, B. D., Hossaini, R., et al. (2014). Ozone-depleting substances (ODSs) and other gases of interest to the Montreal protocol, Chapter 1. In *Scientific assessment of ozone depletion: 2014*, *Global Ozone Research and Monitoring Project – Report No. 55* (105 pp.). Geneva, Switzerland: World Meteorological Organization.

Chen, D., Huey, L. G., Tanner, D. J., Salawitch, R. J., Anderson, D. C., Wales, P. A., et al. (2016). Airborne measurements of BrO and the sum of HOBr and Br_2 over the tropical West Pacific from 1 to 15 km during the CONvective TRansport of active species in the tropics (CONTRAST) experiment. *Journal of Geophysical Research: Atmospheres*, *121*, 12,560–12,578. https://doi.org/10.1002/2016JD025561

Ehhalt, D. H., Rohrer, F., Blake, D. R., Kinnison, D. E., & Konopka, P. (2007). On the use of nonmethane hydrocarbons for the determination of age spectra in the lower stratosphere. *Journal of Geophysical Research*, *112*, D12208. https://doi.org/10.1029/2006JD007686

Hall, S. (2015). NSF/NCAR GV HIAPER Atmospheric Radiation Package (HARP) CCD Actinic Flux Spectrometers Photolysis Frequencies. Version 1.0. UCAR/NCAR – Earth Observing Laboratory. https://doi.org/10.5065/D6N29V08, Accessed 15 July 2018.

Hall, T. M., & Plumb, R. A. (1994). Age as a diagnostic of stratospheric transport. *Journal of Geophysical Research*, *99*, 1059–1070. https://doi.org/10.1029/93JD03192

Holzer, M., & Hall, T. M. (2000). Transit-time and tracer-age distribution in geophysical flows. *Journal of the Atmospheric Sciences*, *57*, 3539–3558. https://doi.org/10.1175/1520-0469

Holzer, M., & Waugh, D. W. (2015). Interhemispheric transit time distributions and path-dependent lifetimes constrained by measurements of SF6, CFCs, and CFC replacements. *Geophysical Research Letters*, *42*, 4581–4589. https://doi.org/10.1002/2015GL064172

Hossaini, R., Chipperfield, M. P., Monge-Sanz, B. M., Richards, N. A. D., Atlas, E., & Blake, D. R. (2010). Bromoform and dibromomenthane in the tropics: A 3-D model study of chemistry and transport. *Atmospheric Chemistry and Physics*, *10*, 719–735. https://doi.org/10.5194/acp-10-719-2010

Houze, R. A. Jr. (1993). *Cloud dynamics* (p. 573). San Diego, CA: Academic Press.

Houze, R. A. Jr. (2014). *Cloud dynamics* (2nd ed., p. 423). Oxford, UK: Elsevier/Academic Press.

Johnson, J. E. (1981). The lifetime of carbonyl sulfide in the troposphere. *Geophysical Research Letters*, *8*, 938–940. https://doi.org/10.1029/GL008i008p00938

Johnson, R. H., Ciesielski, P. E., & Rickenbach, T. M. (2016). A further look at Q_1 and Q_2 from TOGA COARE. Multiscale convection-coupled systems in the tropics: A tribute to Dr. Michio Yanai, Chap. 1. *Meteorological Monographs*, *56*, 1.1–1.12. https://doi.org/10.1175/AMSMONOGRAPHS-D-15-0002.1

Koenig, T. K., Volkamer, R., Baidar, S., Dix, B., Wang, S., Anderson, D. C., et al. (2017). BrO and inferred Br_y profiles over the western Pacific: Relevance of inorganic bromine sources and a Br_y minimum in the aged tropical tropopause layer. *Atmospheric Chemistry and Physics*, *17*, 15,245–15,270. https://doi.org/10.5194/acp-17-15245-2017

Konopka, P., Ploeger, F., Tao, M., & Riese, M. (2017). Regionally resolved diagnostic of transport: A simplified forward model for CO_2. *Journal of the Atmospheric Sciences*, *74*, 2689–2700. https://doi.org/10.1175/JAS-D-16-0367.1

Krysztofiak, G., Catoire, V., Hamer, P. D., Marécal, V., Robert, C., Engel, A., et al. (2018). Evidence of convective transport in tropical West Pacific region during SHIVA experiment. *Atmospheric Science Letters*, *19*, e798. https://doi.org/10.1002/asl.798

Li, F., Waugh, D. W., Douglass, A. R., Newman, P. A., Pawson, S., Stolarski, R. S., et al. (2012). Seasonal variations of stratospheric age spectra in the Goddard Earth Observing System Chemistry Climate Model (GEOSCCM). *Journal of Geophysical Research*, *117*, D05134. https://doi.org/10.1029/2011JD016877

Luo, Z. J., Liu, G. Y., & Stephens, G. L. (2010). Use of A-Train data to estimate convective buoyancy and entrainment rate. *Geophysical Research Letters*, *37*, L09804. https://doi.org/10.1029/2010GL042904

Manion, J. A., Huie, R. E., Levin, R. D., Burgess Jr., D. R., Orkin, V. L., Tsang, W., et al. (2015). NIST Chemical Kinetics Database, NIST Standard Reference Database 17, Version 7.0 (Web Version), Release 1.6.8, Data version 2015.09. Gaithersburg, MD: National Institute of Standards and Technology. Retrieved from http://kinetics.nist.gov/

Masunaga, H., & Luo, Z. J. (2016). Convective and large-scale mass flux profiles over tropical oceans determined from synergistic analysis of a suite of satellite observations. *Journal of Geophysical Research: Atmospheres*, *121*, 7958–7974. https://doi.org/10.1002/2016JD024753

Nicely, J. M., Anderson, D. C., Canty, T. P., Salawitch, R. J., Wolfe, G. M., Apel, E. C., et al. (2016). An observationally constrained evaluation of the oxidative capacity in the tropical western Pacific troposphere. *Journal of Geophysical Research: Atmospheres*, *121*, 7461–7488. https://doi.org/10.1002/2016JD025067

Orbe, C., Holzer, M., Polvani, L. M., & Waugh, D. (2013). Air-mass origin as a diagnostic of tropospheric transport. *Journal of Geophysical Research: Atmospheres*, *118*, 1459–1470. https://doi.org/10.1002/jgrd.50133

Orbe, C., Yang, H., Waugh, D. W., Zeng, G., Morgenstern, O., Kinnison, D. E., et al. (2018). Large-scale tropospheric transport in the chemistry climate model initiative (CCMI) simulations. *Atmospheric Chemistry and Physics*, *18*(10), 7217–7235. https://doi.org/10.5194/acp-18-7217-2018

Ordonez, C., Lamarque, J.-F., Tilmes, S., Kinnison, D. E., Atlas, E. L., Blake, D. R., et al. (2012). Bromine and iodine chemistry in a global chemistry-climate model: Description and evaluation of very short-lived oceanic sources. *Atmospheric Chemistry and Physics*, *12*, 1423–1447. https://doi.org/10.5194/acp-12-1423-2012

Pan, L. L., Atlas, E. L., Salawitch, R. J., Honomichl, S. B., Bresch, J. F., Randel, W. J., et al. (2017). The convective transport of active species in the tropics (CONTRAST) experiment. *Bulletin of the American Meteorological Society*, *98*, 106–128. https://doi.org/10.1175/BAMS-D-14-00272.1

Ploeger, F., & Birner, T. (2016). Seasonal and inter-annual variability of lower stratospheric age of air spectra. *Atmospheric Chemistry and Physics*, *16*, 10,195–10,213. https://doi.org/10.5194/acp-16-10195-20

Schoeberl, M. R., Douglass, A. R., Polansky, B., Boone, C., Walker, K. A., & Bernath, P. (2005). Estimation of stratospheric age spectrum from chemical tracers. *Journal of Geophysical Research*, *110*, D21303. https://doi.org/10.1029/2005JD006125

Schoeberl, M. R., Sparling, L. C., Jackman, C. H., & Fleming, E. L. (2000). A Lagrangian view of stratospheric trace gas distributions. *Journal of Geophysical Research*, *105*, 1537–1552. https://doi.org/10.1029/1999JD900787

SPARC (2013). SPARC report on the lifetimes of stratospheric ozone-depleting substances, Their Replacements, and Related Species. In M. Ko, P. Newman, S. Reimann, & S. Strahan (Eds.), *SPARC Report No. 6, WCRP=15/2103*.

SPARC (2016). SPARC Report on the Mystery of Carbon Tetrachloride. In Q. Liang, P. A. Newman, & S. Reimann (Eds.), *SPARC Report No. 7, WCRP-13/2016*.

Stephens, G. L. (2005). Climate feedbacks in the climate system: A critical review. *Journal of Climate*, *18*, 237–273. https://doi.org/10.1175/JCLI-3243.1

Takahashi, H., & Luo, Z. (2012). Where is the level of neutral buoyancy for deep convection? *Geophysical Research Letters*, *39*, L15809. https://doi.org/10.1029/2012GL052638

Toon, O. B., Maring, H., Dibb, J., Ferrare, R., Jacob, D. J., Jensen, E. J., et al. (2016). Planning, implementation, and scientific goals of the studies of emissions and atmospheric composition, clouds, and climate coupling by regional surveys ($SEAC^4RS$) field mission. *Journal of Geophysical Research: Atmospheres*, *121*, 4967–5009. https://doi.org/10.1002/2015JD024297

Wales, P. A., Salawitch, R. J., Nicely, J. M., Anderson, D. C., Canty, T. P., Baidar, S., et al. (2018). Stratospheric injection of brominated very short-lived substances: Aircraft observations in the Western Pacific and representation in global models. *Journal of Geophysical Research: Atmospheres*, *123*, 5690–5719. https://doi.org/10.1029/2017JD027978

Waugh, D. W., & Hall, T. M. (2002). Age of stratospheric air: Theory, observations, and models. *Reviews of Geophysics*, *40*(4), 1010. https://doi.org/10.1029/2000RG000101

Yanai, M., Esbensen, S., & Chu, J.-H. (1973). Determination of bulk properties of tropical cloud clusters from large scale heat and moisture budgets. *Journal of the Atmospheric Sciences*, *30*, 611–627. https://doi.org/10.1175/1520-0469(1973)030<0611:DOBPOT>2.0.CO;2